

Revisiting l_p -constrained Softmax Loss: A Comprehensive Study

Chintan Trivedi*, Konstantinos Makantasis, Antonios Liapis
and Georgios Yannakakis

Institute of Digital Games, University of Malta, Malta.

*Corresponding author(s). E-mail(s): ctriv01@um.edu.mt;

Abstract

Normalization is a vital process for any machine learning task as it controls the properties of data and affects model performance at large. The impact of particular forms of normalization, however, has so far been investigated in limited domain-specific classification tasks and not in a general fashion. Motivated by the lack of such a comprehensive study, in this paper we investigate the performance of l_p -constrained softmax loss classifiers across different norm orders, magnitudes, and data dimensions in both proof-of-concept classification problems and real-world popular image classification tasks. Experimental results suggest collectively that l_p -constrained softmax loss classifiers not only can achieve more accurate classification results but, at the same time, appear to be less prone to overfitting. The core findings hold across the three popular deep learning architectures tested and eight datasets examined, and suggest that l_p normalization is a recommended data representation practice for image classification in terms of performance and convergence, and against overfitting.

Keywords: classification, normalization, deep learning, computer vision

1 Introduction

Visual content representation in appropriate vector spaces is a fundamental task for any computer vision application [1]. Way before the era of deep learning, computer vision researchers predominately represented visual content by

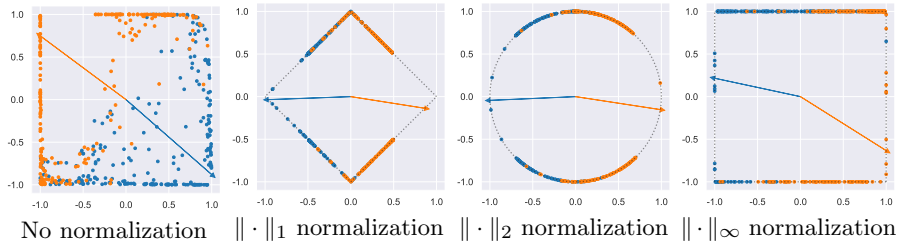
2 Revisiting l_p -constrained Softmax Loss

Fig. 1 Projection of points belonging to two classes (orange or blue) on manifolds using norms of order 1, 2, and ∞ along with the weight vectors for each class (normalized for visualization purposes). Blue points occupy the first and third quadrants, while orange points layer the second and fourth. The points are classified using a neural network with two hidden layers with 16 and 2 neurons respectively and hyperbolic tangent activations. The points' representation is being projected on the manifolds is the 2D output of the second hidden layer.

a set of handcrafted features exploiting the content's local and global properties as well as images' low-level information [2–4]. Although the handcrafted representations were well-defined and their statistical properties were known *a priori*, they were computed independently of the subsequent processing and decision making steps. This gap of information flow—combined with no prior knowledge of which features are best suited for a specific computer vision task—often led to poor performance.

Thanks to the advancements of deep learning, and specifically Convolutional Neural Networks (ConvNets) and Vision Transformers (ViT), the aforementioned gap of information flow has been eliminated. ConvNets and ViT process visual information in its raw form (i.e. images) and learn to extract the most appropriate feature set for a given decision making task [5, 6]. The fact that deep learning automates the visual content representation task has led to breakthroughs in fundamental computer vision tasks such as image classification based on visual information [7]. The computed features, however, are depended on the parameterization of the employed deep learning architectures, the available training data, and the employed loss function. Therefore, the statistical properties, let alone the physical interpretation, of the features computed are barely known. Having no control over the properties of the features may lead to learning machines characterized by poor generalization capacity or misleading predictions [8].

Several approaches have been proposed to control the properties of the computed features such as Batch Normalization [9], Layer Normalization [10], and l_2 -constrained softmax loss [11]. Although the first two are well-established and widely adopted techniques, the latter approach has received limited attention. To the best of our knowledge, l_2 -constrained softmax loss has been introduced and applied only to a few domain-specific studies such as face verification [12, 13], while its effect on the performance of learning machines has not been investigated comprehensively and in a general fashion.

Motivated by the lack of a thorough study on l_p normalization, this paper investigates the impact of l_p -constrained softmax loss—a generalization of l_2 —on the performance of learning machines as applied to the general problem of image classification. The l_p -constrained softmax loss projects the feature representations of data points (e.g. images) on the surface of a manifold with fixed radius; i.e. the magnitude of the l_p norm of the feature representations equals a fixed and predefined number.

In this study, we investigate the effect of this projection on classification performance in terms of three core manifold properties: the order of the norm, the manifold dimension and its radius. Our evaluation builds on a proof-of-concept example that aims to shed light on the behaviour of l_p -constrained softmax loss, and proceeds with the application of l_p -constrained softmax loss on eight publicly available and widely-used image classification datasets. For the evaluation of l_p -constrained softmax loss we use three popular deep learning architectures: two ConvNet architectures and one ViT. Employment of l_p -constrained softmax loss consistently improves the performance of ConvNets. The ViT architecture, however, seems to benefit more when l_p -constrained softmax loss is used with datasets that consist of a large number of classes. Based on the outcomes of our experiments we can argue that l_p -constrained softmax loss can improve the performance of image classification, it leads to faster convergence and protects training against overfitting, and it can be used in conjunction with other normalization techniques; it is, thus, recommended as a general good machine learning practice in that domain.

2 Background: Normalization

As mentioned earlier, the representations of data affect both the performance (generalization capacity) and the behaviour (convergence time, robustness to different initialization) of machine learning models. Therefore, controlling the properties of data representations is essential for successfully addressing pattern recognition tasks. In the following, we review core methods for controlling the properties of data representations that have been designed for and applied to neural network learning models.

One of the first approaches for controlling the statistical properties of data representations has been proposed in [9] and is known as *batch normalization*. As the name suggests, batch normalization standardizes the features (representation elements) across a batch of data points by removing the mean and scaling to unit variance. Batch normalization reduces convergence time, by reducing internal covariance shift [14] and bounding the magnitude of the gradients, and improves networks performance [9].

In contrast to batch normalization, which standardizes the features across batches of data, the authors in [10] suggest standardizing data representations individually. This technique is known as *layer normalization* and results in zero mean and unit variance representations. Layer normalization does not depend

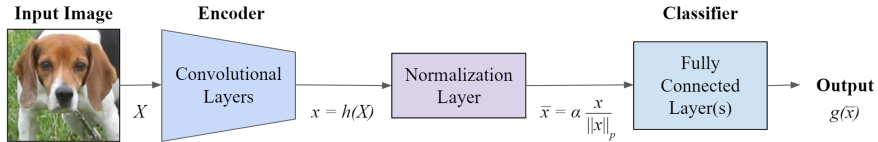
4 Revisiting l_p -constrained Softmax Loss

Fig. 2 Information flow through a ConvNet that uses l_p -constrained softmax loss.

on the batch size, and in the case of recurrent neural networks, it yields more accurate networks than those featuring batch normalization [15, 16].

In addition to batch and layer normalization, *instance normalization* [17] has explicitly been designed and proposed for computer vision tasks and ConvNets. It is applied on third-order tensor objects and standardizes them across two of the three dimensions, i.e. zero mean and unit variance tensor slices. This technique has been devised for style transfer applications [18], and usually it is applied along the spatial dimension of images to produce contrast-agnostic neural network models. A modification of instance normalization known as *group normalization* [19] is also used with third-order tensor objects: instead of standardizing tensor slices, as the name suggests, it standardizes groups of tensor slices.

Instead of manipulating the statistical properties (mean and variance) of representations, another way to control their form is by requiring them to lie onto a specific manifold. Towards this direction, the studies in [11, 20] force the data points' representations to lie on the surface of a unit hypersphere, i.e. the l_2 norm of representations equals one. This way, the representations' direction is retained, while their magnitude is always clipped to one yielding scale-invariant learning models. This approach, also known as *l_2 -constrained softmax loss*, has proved to be beneficial for a number of applications including face verification and identification [12, 21], training auto-encoders [22, 23] and contrastive learning [24].

Batch, layer, instance and group normalization techniques are mainly used to stabilize training and improve convergence rate by reducing variance across batches of data points or individual instances as studied in [25]. These techniques have been widely adopted by the research community and are ubiquitous in modern neural network applications. On the contrary, projecting the representations on the surface of a manifold has not been given the necessary attention yet as there are only limited studies proposing the use of this normalization type. In the current study, we aim to shed light on the effect of this technique on general image classification tasks in a comprehensive manner.

The novelty of this study is four-fold. First, we follow a thorough sensitivity analysis and investigate the behaviour of l_p -constrained softmax loss—a generalization of projecting representations in the surface of a hypersphere—in relation to the manifold's shape, dimension and radius. While l_2 -constrained softmax loss has been studied in the literature sporadically, to the best of our knowledge this is the first time a study examines the effect of different norm

orders (determining the shape of the manifold) on the performance of classifiers. Second, we quantify the impact of l_p -constrained softmax loss holistically: not only in terms of classification accuracy, but also in terms of classes' compactness, and in terms of its deviation from the optimal Bayes classifier. Third, we investigate the stability of l_p -constrained softmax loss classifiers on training and their robustness to overfitting via a proof-of-concept example that is easy to visualise and analyse. Finally, we conduct comprehensive experiments using eight widely-used datasets and three popular deep learning architectures to study the behaviour and impact of l_p -constrained softmax loss on real-world image classification tasks.

At this point we should mention that batch, layer and instance normalization can be applied to any layer of a neural network. On the contrary, l_p -constrained softmax loss operates only on the activations of the layer that produces the image representation to manipulate the manifold onto which the representation is projected. Therefore, we should stress out and clarify that l_p -constrained softmax loss can be used in conjunction and is complementary to other normalization techniques. In fact, in Section 5 we present the performance of l_2 -constrained softmax loss classifiers when applied in conjunction with neural network architectures that employ batch and layer normalization.

The remainder of the paper is organized as follows: Section 3 briefly presents the mathematical formulation of l_p -constrained softmax loss classifiers, Section 4 describes the experimental framework followed in this study. The experimental evaluation of l_p -constrained softmax loss classifiers is reported in Section 5, and Section 6 concludes this work.

3 l_p -constrained Softmax Loss

In typical image classification tasks, machine learning models are trained to classify a given image to its correct category. Let us denote as $\mathcal{X} \subset \mathbb{R}^{c \times h \times w}$ the input space of images with c channels, height h and width w , and as $\mathcal{Y} = \{1, 2, \dots, K\}$ the corresponding class categories. The objective of a machine learning model is to compute a function $f : \mathcal{X} \rightarrow \mathcal{Y}$ that maps an image $X \in \mathcal{X}$ to its corresponding category $y \in \mathcal{Y}$.

In the case of ConvNets and ViT models the function f can be seen as a composition of functions $h : \mathcal{X} \rightarrow \mathbb{R}^d$ and $g : \mathbb{R}^d \rightarrow \mathcal{Y}$. Function h produces the feature representation of images, that is the output of model's penultimate layer, and function g is the classifier that maps the representation $\mathbf{x} = h(X)$ of an image X to a class category, i.e.

$$g(x) = \arg \max_{i \in \mathcal{Y}} (W_i^T h(X) + b_i), \quad (1)$$

where W_i is the i -th column of the model's output weights and b_i the i -th element of the model's output bias vector. Both W_i and b_i are used to compute the output for the i -th class. By examining Eq. (1) it becomes clear that the

predictions of a ConvNet or a ViT are determined by the value of

$$\langle W_i, h(X) \rangle = \|W_i\|_2 \cdot \|h(X)\|_2 \cdot \cos \theta, \quad (2)$$

where θ is the angle between W_i and $h(X)$ and $\|\cdot\|_2$ stands for the second norm of a vector. Therefore, the predictions are depended on the magnitudes of W_i and $h(X)$.

The parameters of the model presented above—that is the parameters of $f = g \circ h$ —are estimated during training by minimizing the empirical softmax loss

$$L = -\frac{1}{M} \sum_{m=1}^M \log \frac{\exp(W_{y_m}^T h(X_m) + b_i)}{\sum_{k=1}^K \exp(W_k^T h(X_m) + b_k)} \quad (3)$$

over a training set $\mathcal{D} = \{(X_m, y_m)\}_{m=1}^M$ of M image-category pairs.

The authors in [12] observed that training a model using the softmax loss function of Eq. (3) and letting $h(X)$ unrestricted encourages the network to learn high magnitude representations for well separated samples and ignore hard to classify samples, which deteriorates the generalization capacity of the classifier. This observation is also formalized in Proposition 1 in [13]. To avoid this drawback, the authors of [12, 13] normalize $h(X)$ such that its second norm is equal to a constant α .

In this work we study a more general normalization technique; specifically, we restrict the p -th norm of $h(X)$ to be equal to a constant α . This way the normalized representation \bar{x} of an image X is given by

$$\bar{x} = \alpha \frac{h(X)}{\|h(X)\|_p}. \quad (4)$$

We investigate the impact of Eq. (4) on the performance of a classifier for different values of p and α , which can be fixed by the user or treated as learnable parameters that are being estimated during the training of the network. The value of p in Eq. (4) affects, first, the shape of the manifold on which $h(X)$ is projected and, second, the value of $\|\bar{x}\|_2$ in Eq. (2). Specifically, let

$$C_p = \frac{\|h(X)\|_2}{\|h(X)\|_p}, \quad (5)$$

then for different values of p , the value of $\|\bar{x}\|_2$ lies in the following interval

$$\frac{\|\bar{x}\|_2}{\alpha} \in [\min(1, C_p), \max(1, C_p)]. \quad (6)$$

Note that $C_2 = 1$ (when $p = 2$) and thus $\|\bar{x}\|_2$ equals to α .

Figure 1 presents the projection of $h(\mathbf{x})$ for $\mathbf{x} \in \mathbb{R}^2$ for $p = 1, 2$ and ∞ . The points depicted belong to one of two classes: blue and orange. Blue points occupy the first and third quadrants in a 2D Euclidean space and orange points

the second and fourth. The points are classified using a neural network with two hidden layers with 16 and 2 neurons respectively, and hyperbolic tangent activations. The representation of points projected on manifolds is the 2D output of the networks' hidden layer. Figure 2 presents the information flow for a ConvNet that employs this kind of normalization, which can be easily implemented using built-in functions from publicly available deep learning toolboxes such as Tensorflow [26], Caffe [27] and Pytorch [28].

4 Experimental Framework

In this section we present the experimental framework used for investigating the impact of l_p -constrained softmax loss on the performance of neural network classifiers. We start by introducing the employed datasets and models. Then, we define the experimental setting and the metrics used for evaluating models' performance.

4.1 Datasets

We employ both synthetic and real-world datasets. Using synthetic data, we formulate a proof-of-concept problem for studying the robustness and generalization capacity of neural network classifiers that utilizes l_p -constrained softmax loss (see Section 4.1.1). Complementary to synthetic data we use eight different real-world datasets—corresponding to dissimilar image classification tasks—and three popular deep learning architectures to evaluate the performance of l_p -constrained softmax loss classifiers in a comprehensive fashion (see Section 4.1.2).

4.1.1 Proof-of-concept dataset

Instead of using only real-world datasets, we also investigate the behaviour of l_p -constrained softmax loss classifiers on a proof-of-concept problem using synthetic data. Through synthetic data we can both visualize the classifiers' decision boundary and test their generalization capacity by comparing them against the optimal Bayes classifier. The latter is possible since the Bayes classifier is defined in terms of the data generating distribution, which is known.

The synthetic dataset consists of 500 two dimensional points that belong to two classes, i.e. binary classification in 2D Euclidean space. Each class consists of 250 points generated by a Mixture of two Gaussian components. For the first class the means of the components are $(-1.5, 1.5)$ and $(1.5, -1.5)$, while for the second class are $(-1.5, -1.5)$ and $(1.5, 1.5)$. All components have the same contribution—equal to 0.5—to the mixtures and their covariance is the diagonal matrix $\text{diag}([1.2, 1.2])$. According to this data generating distribution, all points of the first class are assigned to the first and third quadrants whereas and the points of the second class are placed onto the second and fourth. For this dataset, all models share the same architecture and their weights have been initialized using the same set of values. Moreover, we train all of them using the same set of data.

Dataset	Classes	Im. Size	Train	Val	Batch
beans	3	224x224	1034	133	64
cats vs dogs	2	128x128	19,773	3,489	64
cifar10	10	32x32	50k	10K	128
cifar100	100	32x32	50k	10K	128
imagenette	10	128x128	9,469	3,925	64
rock paper scissors	3	224x224	2,520	372	32
stanford dogs	120	128x128	12K	8,580	64
tf flowers	5	224x224	3,103	547	32

Table 1 Summary of datasets used and the respective training hyper-parameters.

4.1.2 Real-world datasets

We evaluate the performance of l_p -constrained softmax classifiers across eight (8) publicly available datasets, see Table 1, from the Tensorflow Datasets Catalog¹. All eight datasets are widely used for benchmarking machine learning models on image classification tasks.

The selection of the datasets to be examined is based on two core criteria. First, we choose to use datasets of varying *size*; small-sized containing less than 10K images, medium-sized with 10K-25K images and large datasets with more than 25k images. Using varying size datasets, we can test the generalization capacity of the l_p -constrained softmax classifiers and their behaviour against overfitting. Second, we chose datasets with a varying number of *classes*. As shown in [29], softmax loss is affected by the number of classes due to the normalization factor (see the denominator in Eq.(3)). Based on that, we selected datasets whose classes range from 2 to 120. This way, we can investigate the degree to which discriminating class weight vectors can be learnt on manifolds of specific shape and size when the number of classes changes. Moreover, we can measure the compactness of class-wise clusters formed on the representation space given that the normalized points (see Eq.(6)) should ideally form compact clusters based on their corresponding class labels. Finally, to increase the datasets’ size, we used data augmentation techniques, including random horizontal flip, rotation and scaling of the images [30].

4.2 Models

For the proof-of-concept problem we use a fully connected neural network with two hidden layers and hyperbolic tangent activations. The l_p normalization is applied to the output of the second hidden layer. The first hidden layer consists of 128 neurons, while the number of neurons at the second hidden layer ranges from 2 to 16 to test the effect of the representation’s dimension on the model’s performance.

For the real-world datasets, instead, we use the ResNet50 as an encoder that maps images to a 2,048 dimension space. The ResNet50 encoder is followed by a dense layer that is responsible for carrying out the classification task. We use ResNet50 since it is a widely-used mid-sized (~ 25 M parameters) ConvNet that achieves excellent performance in general image classification tasks. We train

¹www.tensorflow.org/datasets/catalog/overview#image_classification

the encoder and the subsequent classification layer in an end-to-end fashion without using pre-trained weights to enable the network to learn appropriate l_p normalized representations of the images. At this point, we should stress that we do not aim to produce state-of-the-art results on the datasets presented above. Instead, our aim is to examine whether the l_p normalization can boost the performance of an image classifier.

4.3 Experiments and Metrics

For all datasets we run experiments investigating the effect of the l_p normalization hyperparameters, that is p and α in Eq. (6). These hyperparameters can be determined in advance, or become learnable parameters that are estimated during the classifier’s training. Specifically, we test four different settings for parameter p ($p = 1, 2, \infty$ and learnable) and two for parameter α ($\alpha = 1$ and learnable).

For each hyperparameter setting in the real-world datasets, we run five separate experiments with different Glorot-Uniform weight initializations and random data augmentation to test the robustness of the models. We evaluate the effect of l_p normalization on the performance of the models using a set of metrics. For the proof-of-concept problem—since the data generating distribution is known—we use the trained classifier’s deviation from the Bayes optimal classifier; i.e. the probability that predictions of the trained classifier and the Bayes classifier are different when a point is randomly sampled from the data generating distribution. For the real-world datasets, we use the validation accuracy and the evolution of training loss. These are typical classification metrics, which also allow testing a classifier’s behaviour in terms of overfitting. We also use the silhouette score [31] to quantify the compactness of class-wise clusters produced by l_p normalized image representations.

5 Results

This section evaluates the impact of l_p -constrained softmax loss on models’ performance following the experimental framework described earlier in Section 4. We start by presenting the results for the proof-of-concept problem and move on with the results obtained on the real-world data².

5.1 Proof-of-concept problem

Running experiments using the proof-of-concept data and models described in Section 4 allows us to investigate the behaviour of l_p -constrained softmax loss classifiers in terms of their decision boundaries as well as their deviation from the optimal Bayes classifier.

Figure 3 presents the decision boundaries for different parameterized l_p -constrained softmax loss classifiers and the boundary for a classifier that does not use any normalization. For these results, we use the model described in

²The code is available at <https://github.com/ChintanTrivedi/LpSoftmaxLoss>

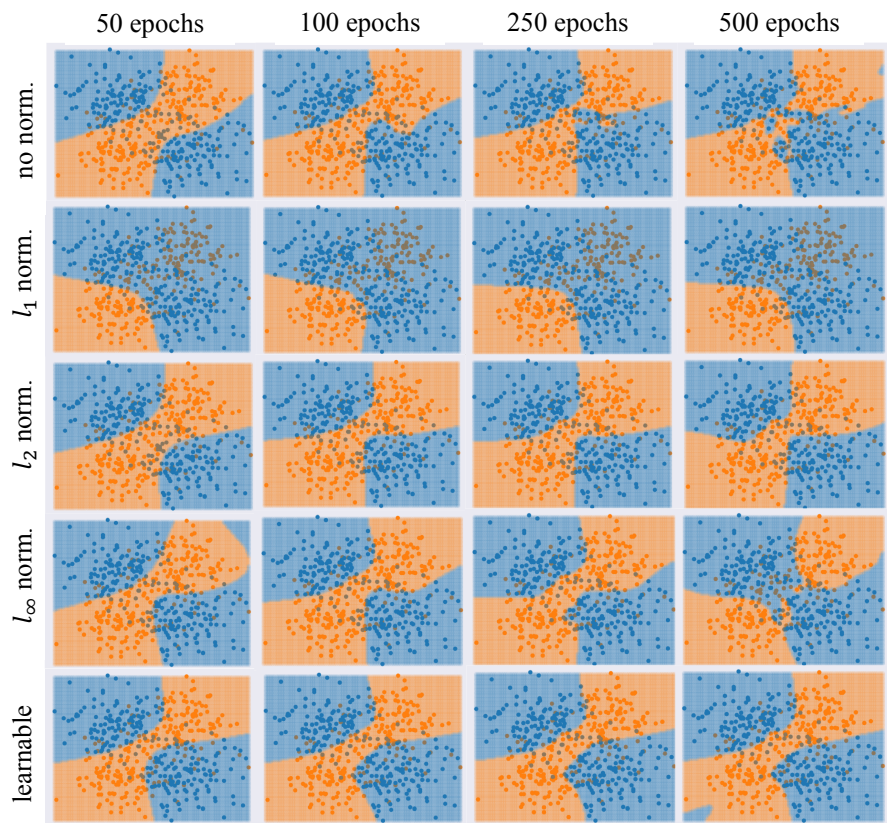


Fig. 3 Decision boundaries for classifiers using l_p normalization on the proof-of-concept data.

Section 4 with two neurons at its penultimate layer—we apply l_p normalization to 2D data representations.

The classifier that does not use any normalization produces good decision boundaries when the training time is appropriately set; i.e. 100 epochs. If we over-train the classifier, however, it starts overfitting the data after 250 epochs and it becomes more apparent at 500 training epochs. On the contrary, the decision boundary of l_p constrained softmax loss classifiers, when p is learnable and $p = 2$, does not seem to be affected by over-training. These models learn accurate decision boundaries and retain them independently of training time. The classifier that uses l_∞ normalization behaves similar to the classifier that does not use any normalization; its decision boundary is accurate, but it is not robust to over-training. Finally, the classifier that employs l_1 normalization underfits the data regardless of the number of training epochs used. These results suggest that l_p constrained softmax loss classifiers can learn accurate decision boundaries, and at the same time, they are robust against overfitting.

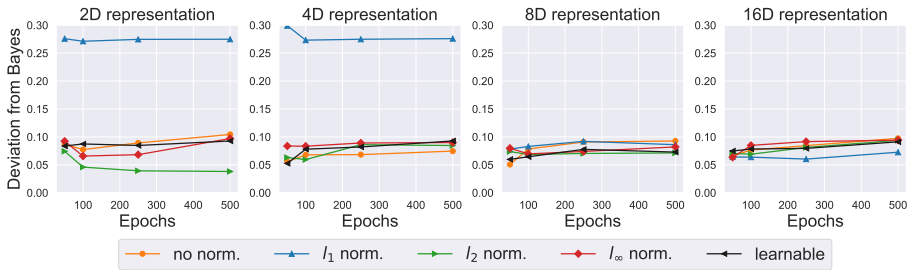


Fig. 4 Deviation from the optimal Bayes classifier.

However, they have to be appropriately parameterized to avoid local minima and underfitting.

In Figure 4 we evaluate more formally the classifiers' performance by measuring their deviation from the optimal Bayes classifier. We also try to relate the behaviour of l_p normalization to the dimension of data representations. Towards this direction, we apply l_p normalization to data representations of varying dimension, i.e. the number of neurons at the penultimate layer of the classifiers is 2, 4, 8, and 16. Deviation from the optimal Bayes decision rule quantifies the models' generalization capacity; low deviation indicates that a model can produce accurate predictions on unseen data, while high deviation suggests that a model either overfits or underfits the data.

The left diagram in Figure 4 corresponds to the decision boundaries presented in Figure 3. The l_2 -constrained softmax loss classifier can learn the most accurate decision boundary without being affected by over-training. All l_p -constrained softmax loss classifiers, except the one that uses l_1 normalization, produce better decision rules than the classifier that does not use any normalization. The same holds for 8-dimensional and 16-dimensional data representations, but, surprisingly, not for the 4-dimensional ones. In this case, the unconstrained classifier that does not use any normalization technique outperforms all other classifiers after 150 epochs of training. Despite that result, we can conclude that the performance of l_p -constrained softmax loss classifiers is affected less by the dimension of data representation.

A surprising result regards the behaviour of the l_1 -constrained softmax loss classifier. For small data representations, it highly underfits the data. When the dimension increases, however, it produces comparable or even better results compared to the other classifiers. The fact that l_1 normalization produces better results with overparameterized models is interesting and needs to be further investigated both experimentally and theoretically.

To summarize, results from the proof-of-concept problem suggest that l_p -constrained softmax loss classifiers—when they are appropriately set in terms of parameter p —are more robust to overfitting and improve classification performance.

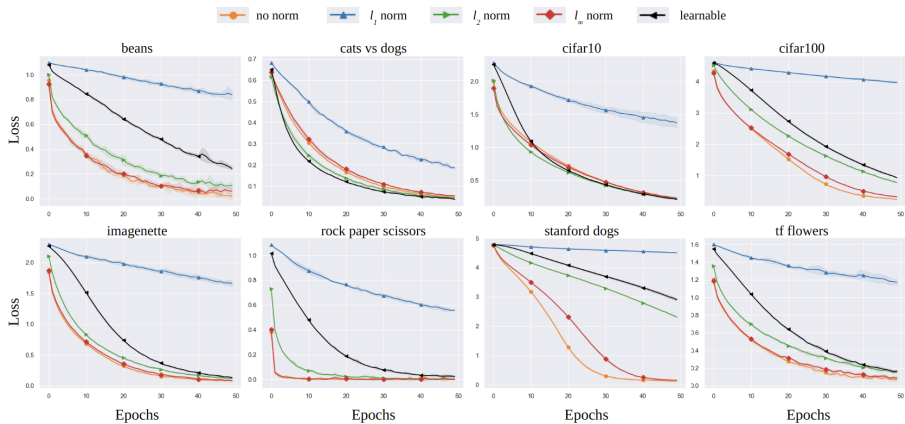


Fig. 5 Progress of training loss for different values of p .

Dataset	No norm	l_1 norm	l_2 norm	l_∞ norm	learnable
beans	81.7 \pm 2.3	65.6 \pm 17.5	84.7 \pm 6.8	75.8 \pm 4.7	82.0 \pm 9.5
cats-vs-dogs	90.2 \pm 0.9	91.1 \pm 1.5	90.9 \pm 1.6	89.9 \pm 3.2	91.1 \pm 0.9
cifar10	69.6 \pm 0.5	41.0 \pm 4.8	71.3 \pm 0.5	69.9 \pm 0.7	72.6 \pm 1.3
cifar100	35.6 \pm 1.0	5.5 \pm 0.9	37.6 \pm 0.7	36.9 \pm 0.3	36.2 \pm 0.7
imagenette	64.6 \pm 1.7	43.9 \pm 4.9	67.8 \pm 2.1	61.2 \pm 4.5	69.0 \pm 2.2
rock-paper-scissors	86.3 \pm 6.3	81.1 \pm 22.9	96.5 \pm 5.7	87.0 \pm 18.6	99.3 \pm 1.3
stanford-dogs	11.3 \pm 1.4	2.8 \pm 0.7	11.4 \pm 1.2	11.8 \pm 1.1	8.7 \pm 0.6
tf-flowers	73.8 \pm 3.2	63.4 \pm 3.0	76.5 \pm 2.8	70.7 \pm 5.3	78.6 \pm 3.4

Table 2 Validation set classification accuracy and corresponding 95% confidence intervals across 5 independent trials for different values of parameter p . Values in bold indicate the highest average accuracy obtained within a dataset.

5.2 Real-world Datasets

In this section we investigate the behaviour of l_p -constrained softmax loss, in terms of its parameters, i.e. p , α and representation dimension, using real-world data.

5.2.1 Varying Orders of Norm (p)

Parameter p corresponds to the order of the norm that is used for normalizing data representations. Following the procedure presented in Section 4, we evaluate classifiers' performance when p is fixed to 1, 2 and ∞ , and when p is a learnable parameter. We compare their performance against a classifier that is not using any normalization technique. Throughout this set of experiments, we use the ResNet model presented in Section 4.2.

Figure 5 presents how training loss changes in the first 50 epochs of training. Solid lines represent the mean loss for five runs and shaded areas show the 95% confidence interval. For all datasets, except *stanford-dogs*, the classifiers converge within 50 training epochs. All classifiers, except l_1 -constrained softmax loss, converge within 50 epochs of training for six out of eight datasets. For the *stanford-dogs* and *cifar100* datasets, the classifiers need more epochs

to converge as these datasets contain many classes and can be considered harder as a machine learning task. As shown in Figure 5, l_p -constrained softmax loss classifiers that have their p parameter appropriately set ($\alpha = 1$ for all experiments) converge faster and, in many cases, to lower loss values than the classifier that is not using any normalization technique. The worst performing l_p -constrained softmax loss classifier is the one that employs l_1 normalization. Actually, l_1 -constrained softmax loss classifier does not manage to converge within 50 epochs of training for none of the eight employed datasets. On the contrary, the classifier that sets $p = \infty$ converges faster than all the other l_p -constrained softmax loss classifiers.

Besides convergence rates, we also investigate the classification accuracy on the validation set (unseen during training), since this is a far more representative metric for evaluating a classifier's performance. Table 2 presents the mean validation accuracies and the corresponding 95% confidence intervals of the models. l_p -constrained softmax loss classifiers generally perform better in most cases than the baseline classifier with no normalization. Specifically, l_2 -constrained softmax loss classifier outperforms the baseline classifier that uses no normalization in all datasets, while in 2 (*cifar10* and *cifar100*) out of 8 datasets its accuracy is significantly higher (based on 95% confidence intervals) than the baseline. The l_∞ -constrained softmax loss classifier outperforms the baseline classifier in 4 out of 8 datasets, and in *cifar100* it performs significantly better than the baseline. When we treat the p parameter as a learnable one, the l_p -constrained softmax loss classifier performs better than the baseline in 7 out of 8 datasets and in 3 of them (*cifar10*, *imagenette* and *roch-paper-scissors*) significantly better. Finally, l_1 -constrained softmax loss classifier achieves better performance than the baseline classifier in only one dataset (*cats-vs-dogs*).

Based on the results obtained so far, we can safely argue that l_p normalization for $p = 2$ or learnable p can boost an image classifier's performance. More importantly, this performance improvement comes for free, without any sophisticated or ambiguous model design choices.

5.2.2 Varying Manifold Scale (α)

In this section we investigate the degree to which the radius (parameter α) of the manifold on which the point representations are projected affects the performance of an l_p -constrained softmax loss classifier. In this set of experiments we again use the ResNet model described in Section 4.2. We run experiments for fixed $\alpha = 1$ and for learnable α , and we use two different classifiers: one that employs l_2 normalization and one that treats p as a learnable parameter. The performance evaluation takes place in terms of classification accuracy on validation sets.

Figure 6 presents the results for this investigation for the two classifiers. While there are some fluctuations in early stages of learning, for 7 out of the 8 employed datasets the final accuracy of the models seems unaffected by the tested α, p parameter sets. For the *stanford-dogs* dataset, however, the classifier

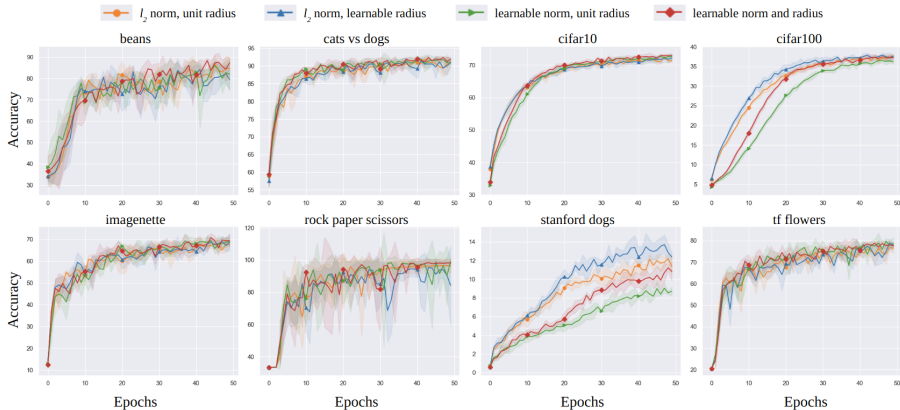


Fig. 6 Progress of validation accuracy for different values of α .

that uses l_2 normalization and learnable α seems to achieve significantly higher accuracy compared to the other parameters settings.

The above finding is in alignment with the results obtained in [12, 13] where the authors relate the parameter α with the number of available classes: the larger the number of classes, the larger the value of α should be. Based on these results, we can conclude that allowing α to be estimated during the model’s training is a safe choice no matter what the number of classes is.

5.2.3 Varying Dimensions of Representation

In the experiments reported thus far, the ResNet model described in Section 4.2 maps images to 2048 dimension vector representations, which then are normalized and propagated to the network’s output via a hidden layer i.e. the classification boundary is non-linear in the space of the normalized representations.

In the following, we investigate how the linearity/non-linearity and complexity—in terms of the number of trainable parameters—of classifiers affect the layout of the learned representations on the manifold. In other words, we investigate the compactness and separability of the classes to which the normalized data representations belong.

We use dense neural networks with one hidden layer and vary the number of hidden neurons to investigate l_p normalization when applied to representations of different dimensions. The quality of normalized representations is evaluated in terms of silhouette score as this metric quantifies the compactness of the classes and their separability on the manifold.

Table 3 presents the silhouette score for nonlinear and linear classifiers. For l_p normalization we used $p = 2$ and $\alpha = 1$ to assure that the radius and the form of the manifold on which the representations are projected are the same for all classifiers. This way, the computed silhouette scores are directly comparable. For all datasets examined, except the *stanford-dogs*, the linear classifier produces the highest silhouette score, on average. Specifically, its

Dataset	Feature Representation Size				
	4096	2048	512	128	0
beans	0.36±0.06	0.38±0.02	0.41±0.06	0.44±0.04	0.49±0.10
cats-vs-dogs	0.46±0.03	0.46±0.01	0.48±0.01	0.48±0.02	0.54±0.02
cifar10	0.11±0.00	0.12±0.00	0.14±0.00	0.16±0.01	0.17±0.00
cifar100	-0.12±0.00	-0.12±0.00	-0.13±0.00	-0.14±0.00	-0.11±0.00
imagenette	0.11±0.02	0.13±0.00	0.14±0.01	0.16±0.03	0.20±0.02
rock-paper-scissors	0.69±0.09	0.63±0.11	0.78±0.05	0.80±0.07	0.86±0.09
stanford-dogs	-0.11±0.01	-0.11±0.00	-0.12±0.00	-0.14±0.01	-0.14±0.01
tf-flowers	0.20±0.02	0.23±0.01	0.23±0.03	0.26±0.03	0.30±0.04

Table 3 Average silhouette scores after 50 epochs for different representation sizes of the penultimate layer. Values are averaged across 5 runs with 95% confidence intervals. Values in bold indicate the highest average silhouette score obtained within a dataset.

silhouette score is significantly higher than when using a nonlinear classifier with 4096 features in 4 datasets, with 2048 features in 5 datasets, with 512 features in 3 datasets, and with 128 features in 1 dataset.

As far as the nonlinear classifier is concerned, we observe that the silhouette score monotonically decreases as we increase the representation’s dimension. For *cifar100* and *stanford-dogs* datasets, however, all classifiers perform equally poorly and the classes overlap in the representation space due to large number of classes. These findings suggest that the simpler the classifier, the better (or at least equal) the quality of the normalized representations on average, in terms of class compactness and separability.

5.2.4 l_p norm normalization and other normalization techniques

In the previous sections, we investigated the behaviour of l_p -constrained softmax loss classifiers in terms of their parameters, that is parameter p representing the norm order and parameter α representing the radius of the manifold on which the data representations are projected. In this section we investigate the degree to which l_p -constrained softmax loss classifiers can be used in conjunction with other data normalization techniques. Specifically, we investigate the behaviour of l_p norm normalization when the classifier employs batch normalization and layer normalization.

To investigate the behaviour of l_p norm normalization in conjunction with batch normalization we use the EfficientNet-B0 [32] architecture, since this model employs batch normalization. While batch normalization is widely used with ConvNets, layer normalization is used with models that take into consideration sequential data. For this reason, we investigate the behaviour of l_p norm normalization using a Vision Transformer (ViT) model, since this model is used for image classification tasks exploiting sequential data and employs layer normalization. Throughout these experiments we set parameter p of the l_p -constrained softmax loss classifiers to 2.

Table 4 presents the classification accuracy on validation sets and corresponding 95% confidence intervals for EfficientNet-B0 and ViT. We compare

Dataset	EfficientNet-B0		Visual Transformer	
	No Norm	l_2 Norm	No Norm	l_2 Norm
beans	76.4 ± 3.9	75.5 ± 5.2	80.5 ± 1.1	82.7 ± 2.4
cats-vs-dogs	85.5 ± 1.2	86.7 ± 0.9	79.5 ± 0.7	79.0 ± 1.9
cifar10	82.0 ± 0.2	83.1 ± 0.7	76.1 ± 0.7	73.6 ± 0.8
cifar100	50.2 ± 0.5	51.3 ± 0.7	46.6 ± 0.9	50.7 ± 0.9
imagenette	62.3 ± 3.3	64.0 ± 1.6	67.7 ± 0.5	65.9 ± 2.1
rock-paper-scissors	80.1 ± 5.1	83.3 ± 6.9	83.7 ± 5.0	65.7 ± 6.0
stanford-dogs	9.1 ± 0.3	11.0 ± 0.4	10.3 ± 0.5	12.0 ± 0.1
tf-flowers	74.3 ± 2.2	74.7 ± 2.7	69.4 ± 1.7	71.5 ± 1.1

Table 4 Validation set classification accuracy and corresponding 95% confidence intervals across 5 independent trials for EfficientNet-B0 and ViT. Values in bold indicate the highest average accuracy obtained within a dataset.

the performance of the models with and without applying l_2 norm normalization. In the case on EfficientNet-B0, which is a popular ConvNet architecture the classification performance improves for 7 out of the 8 datasets and significantly better (based on 95% confidence interval) for 2 of them (*cifar10*, *stanford-dogs*). Therefore, based on these results we conclude that l_2 normalization can be used in conjunction with batch normalization to improve the performance of a ConvNet.

In the case of ViT the results are more balanced. The ViT that employs l_2 norm normalization performs better for 4 out of the 8 datasets, while for 2 of them (*cifar100* and *stanford-dogs*) it performs significantly better. However, similarly, the ViT that does not apply l_2 norm normalization on data representations performs better for 4 out of the 8 datasets, and for 2 of them (*rock-paper-scissors* and *cifar10*) significantly better. Based on these results, we can conclude that in the case of ViT, which employs layer normalization, l_2 norm normalization is beneficial when the number of classes is large. Both *cifar100* and *stanford-dogs* datasets for which the ViT with l_2 norm normalization performs significantly better include data from 100 and 120 classes, respectively.

6 Conclusions

This study evaluates the behaviour of l_p -constrained softmax loss classifiers on a proof-of-concept problem and eight popular real-world image classification tasks. Our experimental results across all tasks examined suggest that l_p normalization—when appropriately parameterized—improves classification performance, leads to faster convergence and shields models against overfitting. Using the second norm ($p = 2$) or treating p as a learnable parameter for normalizing the data appear to produce the most robust results across all experimental settings. The size of the manifold—i.e. parameter α controlling the magnitude of normalized data representations—can affect the classifier’s performance when the employed dataset consists of many classes; this hyperparameter, however, can be estimated during training time. Of particular interest is the behaviour of l_1 normalization when employed on overparameterized data representations. While overparameterization boosts the capacity of learning

models, it also increases the risk for overfitting; l_1 normalization, however, seems to permit the increase in learning capacity without letting the models to overfit. This behaviour needs to be further investigated both experimentally and theoretically. Finally, l_p -constrained softmax loss consistently improves the performance of ConvNet architectures, while the benefits for ViT models are more obvious when the classification task employs a large number of classes.

To conclude, the key findings of this study suggest that l_p normalization improves classification performance in a general fashion, in conjunction with other normalization techniques and for different model architectures by producing classifiers less prone to overfitting. Importantly, l_p normalization can be used without any sophisticated or ambiguous classifier design choices and can be easily implemented using built-in functions from publicly available deep learning toolboxes. The limited set of hyperparameters that define l_p normalization can also be learnable without a loss in performance.

Acknowledgments. This work has been supported by the European Union’s Horizon 2020 research and innovation programme from the TAMED project (Grant Agreement No. 101003397).

References

- [1] Marr, D.: Visual information processing: The structure and creation of visual representations. *Philosophical Transactions of the Royal Society of London. B, Biological Sciences* **290**(1038), 199–218 (1980)
- [2] Tuytelaars, T., Mikolajczyk, K.: *Local Invariant Feature Detectors: a Survey*. Now Publishers Inc, ??? (2008)
- [3] Zheng, L., Yang, Y., Tian, Q.: Sift meets cnn: A decade survey of instance retrieval. *IEEE transactions on pattern analysis and machine intelligence* **40**(5), 1224–1244 (2017)
- [4] Roth, P.M., Winter, M.: *Survey of appearance-based methods for object recognition*. Inst. for computer graphics and vision, Graz University of Technology, Austria, technical report ICGTR0108 (ICG-TR-01/08) (2008)
- [5] LeCun, Y., Bottou, L., Bengio, Y., Haffner, P.: Gradient-based learning applied to document recognition. *Proceedings of the IEEE* **86**(11), 2278–2324 (1998)
- [6] Sharif Razavian, A., Azizpour, H., Sullivan, J., Carlsson, S.: Cnn features off-the-shelf: an astounding baseline for recognition. In: *Proceedings of the IEEE Conference on Computer Vision and Pattern Recognition Workshops*, pp. 806–813 (2014)

- [7] Krizhevsky, A., Sutskever, I., Hinton, G.E.: Imagenet classification with deep convolutional neural networks. *Advances in neural information processing systems* **25**, 1097–1105 (2012)
- [8] Yuan, X., He, P., Zhu, Q., Li, X.: Adversarial examples: Attacks and defenses for deep learning. *IEEE transactions on neural networks and learning systems* **30**(9), 2805–2824 (2019)
- [9] Ioffe, S., Szegedy, C.: Batch Normalization: Accelerating Deep Network Training by Reducing Internal Covariate Shift (2015)
- [10] Ba, J.L., Kiros, J.R., Hinton, G.E.: Layer Normalization (2016)
- [11] Tygert, M., Szlam, A., Chintala, S., Ranzato, M., Tian, Y., Zaremba, W.: Scale-invariant learning and convolutional networks. *arXiv preprint arXiv:1506.08230* (2015)
- [12] Ranjan, R., Castillo, C.D., Chellappa, R.: L2-constrained softmax loss for discriminative face verification. *arXiv preprint arXiv:1703.09507* (2017)
- [13] Wang, F., Xiang, X., Cheng, J., Yuille, A.L.: Normface: L2 hypersphere embedding for face verification. In: *Proceedings of the 25th ACM International Conference on Multimedia*, pp. 1041–1049 (2017)
- [14] Santurkar, S., Tsipras, D., Ilyas, A., Madry, A.: How does batch normalization help optimization? *Advances in neural information processing systems* (31) (2018)
- [15] Xu, J., Sun, X., Zhang, Z., Zhao, G., Lin, J.: Understanding and improving layer normalization. *arXiv preprint arXiv:1911.07013* (2019)
- [16] Vaswani, A., Shazeer, N., Parmar, N., Uszkoreit, J., Jones, L., Gomez, A.N., Kaiser, L., Polosukhin, I.: Attention is all you need. *Advances in Neural Information Processing Systems* **30**, 5998–6008 (2017)
- [17] Ulyanov, D., Vedaldi, A., Lempitsky, V.: Instance normalization: The missing ingredient for fast stylization. *arXiv preprint arXiv:1607.08022* (2016)
- [18] Huang, X., Belongie, S.: Arbitrary style transfer in real-time with adaptive instance normalization. In: *Proceedings of the IEEE International Conference on Computer Vision*, pp. 1501–1510 (2017)
- [19] Wu, Y., He, K.: Group normalization. In: *Proceedings of the European Conference on Computer Vision (ECCV)*, pp. 3–19 (2018)
- [20] Liu, W., Zhang, Y.-M., Li, X., Yu, Z., Dai, B., Zhao, T., Song, L.: Deep hyperspherical learning. *arXiv preprint arXiv:1711.03189* (2017)

- [21] Liu, W., Wen, Y., Yu, Z., Li, M., Raj, B., Song, L.: Spherefacer: Deep hypersphere embedding for face recognition. In: Proceedings of the IEEE Conference on Computer Vision and Pattern Recognition, pp. 212–220 (2017)
- [22] Davidson, T.R., Falorsi, L., De Cao, N., Kipf, T., Tomczak, J.M.: Hyper-spherical variational auto-encoders. arXiv preprint arXiv:1804.00891 (2018)
- [23] Xu, J., Durrett, G.: Spherical latent spaces for stable variational autoencoders. CoRR **abs/1808.10805** (2018) <https://arxiv.org/abs/1808.10805>
- [24] Wang, T., Isola, P.: Understanding contrastive representation learning through alignment and uniformity on the hypersphere. arXiv preprint arXiv:2005.10242 (2020)
- [25] Huang, L., Qin, J., Zhou, Y., Zhu, F., Liu, L., Shao, L.: Normalization Techniques in Training DNNs: Methodology, Analysis and Application (2020)
- [26] Abadi, M., Barham, P., Chen, J., Chen, Z., Davis, A., Dean, J., Devin, M., Ghemawat, S., Irving, G., Isard, M., *et al.*: Tensorflow: A system for large-scale machine learning. In: 12th {USENIX} Symposium on Operating Systems Design and Implementation ({OSDI} 16), pp. 265–283 (2016)
- [27] Jia, Y., Shelhamer, E., Donahue, J., Karayev, S., Long, J., Girshick, R., Guadarrama, S., Darrell, T.: Caffe: Convolutional architecture for fast feature embedding. In: Proceedings of the 22nd ACM International Conference on Multimedia, pp. 675–678 (2014)
- [28] Paszke, A., Gross, S., Massa, F., Lerer, A., Bradbury, J., Chanan, G., Killeen, T., Lin, Z., Gimelshein, N., Antiga, L., *et al.*: Pytorch: An imperative style, high-performance deep learning library. arXiv preprint arXiv:1912.01703 (2019)
- [29] Bamler, R., Mandt, S.: Extreme classification via adversarial softmax approximation. In: International Conference on Learning Representations (2019)
- [30] Shorten, C., Khoshgoftaar, T.M.: A survey on image data augmentation for deep learning. *Journal of Big Data* **6**(1), 1–48 (2019)
- [31] Rousseeuw, P.: Silhouettes: a graphical aid to the interpretation and validation of cluster analysis. *Journal of Computational and Applied Mathematics* **20**, 53–65 (1987)

- [32] Tan, M., Le, Q.: Efficientnet: Rethinking model scaling for convolutional neural networks. In: International Conference on Machine Learning, pp. 6105–6114 (2019). PMLR